Chaotic electron dynamics around a single elliptically shaped antidot

X. Kleber
High Magnetic Field Laboratory CNRS, Boite Postale 166, F-38042 Grenoble, France and INSA-Toulouse, F-31077 Toulouse, France

G. M. Gusev
High Magnetic Field Laboratory CNRS, Boite Postale 166, F-38042 Grenoble, France and Instituto de Fìsica de São Carlos, 13560-970, Universidade de São Paulo, São Paulo, Brazil

U. Gennser
Paul Scherrer Institute, CH-5232 Villigen-PSI, Switzerland

D. K. Maude
High Magnetic Field Laboratory CNRS, Boite Postale 166, F-38042 Grenoble, France

J. C. Portal
High Magnetic Field Laboratory CNRS, Boite Postale 166, F-38042 Grenoble, France and INSA-Toulouse, F-31077 Toulouse, France

D. I. Lubyshev, P. Basmaji, and M. de P.A. Silva
Instituto de Fìsica de São Carlos, 13560-970, Universidade de São Paulo, São Paulo, Brazil

J. C. Rossi
Universidade Federal de São Carlos, São Carlos, Brazil

Yu. V. Nastaushev
Institute of Semiconductor Physics, Russian Academy of Sciences, Siberian Branch, Novosibirsk, Russia
(Received 30 April 1996)

The classical dynamics of a charged particle colliding ballistically around a single antidot in the presence of a magnetic field is studied numerically. This convex billiard allows for the investigation of the stability of the possible orbits, and to test experimentally for the existence of stable orbits. With an elliptically shaped antidot, chaotic and regular trajectories can develop and contribute to the conductivity. By calculating the Poincaré sections and Lyapunov exponents, the dynamics of such a system, and the role played by the regular orbits, is analyzed. A comparison with the experimental result is made, confirming the importance of the geometric shape of the antidots for the transport in an array of artificial scatterers. [S0163-1829(96)04743-1]

I. INTRODUCTION

Magnetotransport in small devices has been intensively investigated over the last decade.[1] Progress in submicrometer lithography has made it possible to study transport in the ballistic regime, where it is mainly governed by the shape of the boundary of the sample. On the other hand, the dynamics of magnetic billiards has been employed to understand classical chaos and its link with quantum chaos.[2] In such systems, the particles are confined in a region of space defined by the boundary, and are free to execute ballistic collision. For certain regular shapes of the billiards (e.g., circular) the system is integrable and the motion is completely predictable. If we deform the circular shape to an elliptical one, the billiard loses its integrability in a magnetic field, and chaos develops in the phase space. Only recently have experiments confirmed the different behavior of regular (circle) and nonregular (stadium) cavities,[3] where a linear and a Lorentzian shape, respectively, have been observed for the weak-localization effect. Magnetotransport studies of arrays of periodic antidots created in a two-dimensional electron gas (2 DEG) have revealed anomalous peaks. To explain such phenomena, the importance of pinned orbit[4,5] and runaway orbits[6,7] has been postulated. The appearance of pinned orbits results in an increase in the longitudinal resistivity, whereas runaway orbits contribute to an increased conductivity. Both have been used to explain the transport anomalies in periodic lattices of circular antidots. Gusev *et al.*[8] have shown that, in a Penrose lattice of antidots, where runaway trajectories cannot exist, the peaks in the resistivity can only be explained by pinned orbits. On the other hand, recent theoretical[7] and experimental work[9] has stressed the importance of runaway trajectories in antidot lattices. However, in our samples and regions of the magnetic field investigated, runaway orbits cannot exist, and therefore play no role in any anomalous magnetoresistance peaks. We will therefore follow the theory for pinned orbits. By calculating Poincaré sections and the velocity correlation function averaged over

the phase space, Fleischmann, Geisel, and Ketzmerick[5] have extracted the fraction of pinned orbits and the resistivity as a function of magnetic field, and compared it to anomalous peaks observed in the magnetoresistance. They suggested that orbits that start in the chaotic sea escape quickly from the antidot, whereas orbits in a regular island do not drift away, even in the presence of an applied electric field. As the conductivity is governed by the chaotic orbits, this leads to a magnetoresistance which depends on the dynamics in the phase space. The key point here is the possibility to obtain a mixture of chaotic and periodic trajectories in the phase space, that can be altered, e.g., by disordering the array of circular antidots.[10]

In the present paper, a rather different situation is investigated—what happens to an electron that collides with an antidot with a size similar to the electron's cyclotron radius. As with the stadium, an elliptically shaped antidot allows for both chaotic and periodic orbits to develop in the phase space, as the electron bounces around the convex surface. The situation is different from both the stadium and the lattice of circular antidots, in that the system is open. The electron trajectory can be followed easily only for as long as it remains trapped by the antidot. When the electron escapes the detailed trajectory depends on the surroundings, making calculations far more complex. This impedes the calculations of the velocity correlation function. Instead, we follow an alternative route in order to understand the behavior of the conductance in this system. If the orbit is stable, an applied electric field will not effect the stability, contrary to the case of a chaotic trajectory, where a small perturbation will lead to the particle escaping from the antidot. To quantify the stability of such orbits, we calculate the corresponding Lyapunov exponent for all the space phase, and compute the fraction of periodic orbits as the magnetic field is changed. We show that for a low value of the Lyapunov exponent, the stable trajectories are not affected by a small electric field, whereas for higher values the resulting drift force ejects the particle from its trajectory around the antidot. The computed fraction of periodic orbits, representing the probability for an incoming particle to remain trapped, allows for a comparison with experimental results. We argue that the fluctuations of this fraction with the magnetic field will manifest itself as an anomalous peak in the magnetoresistance. To confirm this hypothesis, we measured the magnetoresistance of a 2DEG containing a macroscopic number of randomly oriented, elliptical-shaped antidots, and compare the observed fluctuations with the calculations. This shows that the magnetotransport in this type of microstructure is sensitive not only to the form of the antidot lattice, but also to the shapes of the individual antidots.

The rest of the paper is organized as follows. In Sec. II, a billiard model is presented, together with calculations of the Poincaré sections and Lyapunov exponent. The expected response of the electron orbits to an electric field is investigated. In Sec. III the issue of the feasibility of certain experimental realizations is discussed, and numerical calculations are compared with the preliminary experimental results. Finally, in Sec. IV our conclusions are presented.

II. CLASSICAL CHAOS AROUND A SINGLE ANTIDOT

A classical treatment has been successfully used to explain transport in antidot lattices,[4–6,8,11] even for samples where the Fermi wavelength λ_F is close to the antidot size. For ratios between the smallest antidot dimensions (lattice parameter, antidot size, etc.) and λ_F as small as 2, the quantum nature of the carriers does not seem to play a role, since runaway trajectories[11] or pinned orbits[4] can still be identified. Similarly, magnetic billiards have first been analyzed in terms of classical mechanics in order to determine the dynamics in the phase space and thus the classical chaos. Only recently have magnetic billiards and antidot lattices been treated in semiclassical and quantum approaches, in order to obtain complementary information on transport in ballistic cavities and periodic lattices of circular antidots.[3,7,16] Interestingly, the semiclassical approach (when the Fermi wavelength is inferior to the billiard size) based on the periodic orbit theory (or Gutzwiller trace formula) developed by Gutzwiller[12] reveals that the classical trajectories, and more exactly the stability of periodic orbits, also play a large role within this framework. In this work we use a classical treatment based on the identification of periodic orbits, and find that it is adequate to explain transport anomalies. The billiard models have previously worked very well in elucidating the difference in behavior between a regular and a chaotic ballistic cavity, revealing a high sensitivity of the dynamics to the geometric shape of the cavity.[3,16] At the boundaries, the reflections are assumed to be specular, resulting from a hard-wall potential. To study the dynamics of an electron trapped by a single antidot, we assumed the elliptic antidot to be a magnetic billiard, but with several differences compared to previous approaches.[2,13–15,24] In the present calculations the particles collide on the convex side of the boundary, and it is the presence of the magnetic field which forces the electron to remain trapped around the antidot. This model allows us to calculate the stability of the orbit in the phase space by computing the Lyapunov exponent, revealing the different chaotic and regular components of the dynamics. Stable trajectories will not diverge in the phase space as the time evolves, in contrast to chaotic trajectories that fill the whole phase space. An applied electric field can allow a particle moving in a chaotic orbit to escape from the antidot. This prevents us from following the chaotic orbits to infinite times; nevertheless, the calculated number of collisions is directly related to the stability of the orbits, and can readily be related to the experimental situation.

A. Billiard characteristics

The system considered in our study consists of an elliptic, convex billiard with a ratio between the two semiaxes a and b equal to $\beta = a/b = 5$. Without a magnetic field, a particle arriving at the billiard will collide and be reflected away. In the presence of a magnetic field, the charged particle executes cyclotron orbits in such a way that collisions with the boundary can force the particle to remain trapped around the billiard, executing a so-called skipping orbit. By solving the classical equation of motion for a charged particle in crossed electric and magnetic fields, we can follow the time evolution of the trajectories. As in the usual billiard, the phase space can be reduced from four to two dimensions, defined by the variables θ, the angle corresponding to the point of collision, and γ, the angle between the velocity and the tangent to the boundary (see Fig. 1). Assuming a hard-wall

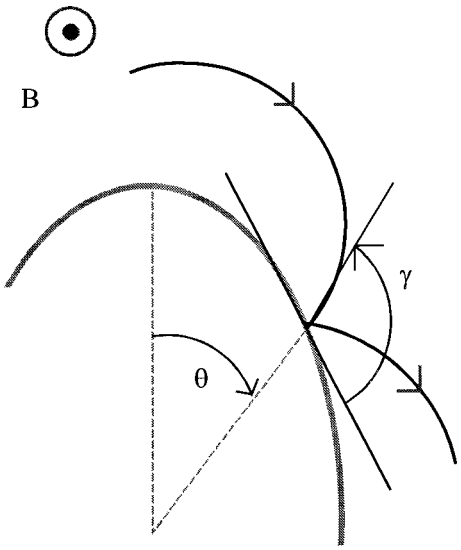

FIG. 1. Geometry of the billiard. The scattering point on the boundary is represented by the angle θ, and γ is the angle between the velocity and the tangent to the boundary. A charged particle in the presence of a magnetic field is assumed to be specularly reflected at the boundary of the billiard.

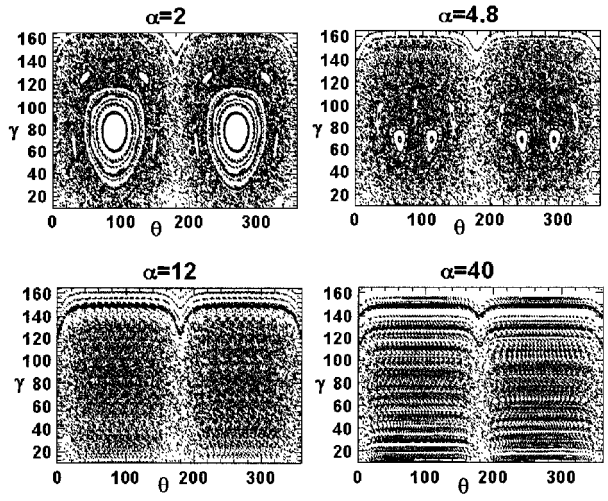

FIG. 2. Poincaré sections for four values of the magnetic field ($\alpha = L/Rc \propto B$). For $\alpha=2$ and $\alpha=4.8$, Poincaré sections exhibit periodic and quasiperiodic orbits surrounded by a chaotic sea. For $\alpha=12$, only the chaotic component remains present, and for larger values of the magnetic field ($\alpha=40$) the system shows a reintrance of integrability. For $\gamma \rightarrow 160°$, the flat segment corresponds to anticlockwise orbits.

potential, the reflections will be specular (the motivation for using the hard-wall potential will be discussed in Sec. II B). For convenience, another set of variables $\{s,p\}$ can be introduced, which are canonically conjugate (thus preserving the Poincaré section area). They are defined by the normalized arclength $s=E(\theta,a,b)$, and the tangential momentum $p=\cos(\gamma)$ [where $E(\theta,a,b)$ is an elliptic integral]. The discrete map is then transformed from $\{\theta(0,360),\gamma(0,180)\}$ to $\{s(0,1),p(-1,1)\}$. In this paper, for clarity, we have retained the variables θ and γ. Defined in this manner the Poincaré section is not area preserving, but it preserves the topology of the phase portrait.[17] The evolution of the dynamics will be controlled by the dimensionless magnetic field $\alpha = L/R_c \propto B$, where L is the length of the ellipse ($L=2a$) and R_c is the cyclotron radius [$Rc=(\hbar/eB)\sqrt{2\pi n_{2D}}$ for a 2 DEG]. Thus each collision at the boundary will be represented by a pair of variables $\{\theta,\gamma\}$ that contains all the information necessary to describe the dynamics of the particle.

B. Poincaré sections

To reduce the complexity of the nonlinear system, it is useful to calculate Poincaré sections. This technique can be used to reduce the dimensionality of the system making the analysis simpler. For a three-dimensional state space, the Poincaré section is generated by choosing a Poincaré plane (a two-dimensional plane) and recording on that surface the points at which a given trajectory cuts though the surface.[18] Generally the choice of the cross section is not primordial and can be chosen, for example, to coincide with a zero value of a dynamical variable. Information about the system can be extracted by looking at the morphology of these Poincaré sections. For a billiard, the situation is somehow different in the sense that the phase space is already a two-dimensional one. Thus a Poincaré map gives a complete description of the phase space.

The Poincaré sections are plotted for different values of the dimensionless magnetic field α. Each intersection between the trajectory and the boundary is represented by a point. Figure 2 shows four Poincaré sections for different values of the magnetic field. For a low value of α, well-defined quasiperiodic orbits appear, characterized by a cycle in the phase space, surrounded by the chaotic component. Increasing the number of points plotted on the Poincaré section will result in the apparition of a single point (elliptic fixed point) in the middle of these cycles, corresponding to a periodic orbit. For a low value of α the region in phase space covered by these quasiperiodic orbits is comparable with the size of the chaotic component, but, as α is increased, only the chaotic part remains. For yet higher values of α the Poincaré section exhibits a more stable dynamics as R_c becomes close or inferior to $\rho_{0\min}$ (minimum radius of curvature of the ellipse).[19] Chaotic components characterized by disconnected points in the state space are reorganized into a more regular structure. Such behavior can be explained by a reentrance of integrability into the system. Of practical importance for the transport properties is the fact that a kind of periodic orbit can develop for a range of value of α and not only for a single one. In addition, near $\gamma=160°$ and independent of α, there exists an invariant curve corresponding to anticlockwise orbits where the particle ''rolls'' around the antidot. Such orbits do not have a physical significance for the transport properties, as the existence of even a small electric field destroys such orbits. In Fig. 3 trajectories corresponding to periodic, chaotic, and anticlockwise orbits are shown schematically. As these orbits play a fundamental role for the determination of the resistivity, we have drawn the most stable periodic orbit that occupies the largest regions in phase space. An important remark is that chaotic trajectories occupy a larger region of real space compared to a regular orbit. Experimentally, this leads to an increase in the probability of a particle executing a chaotic orbit to escape by

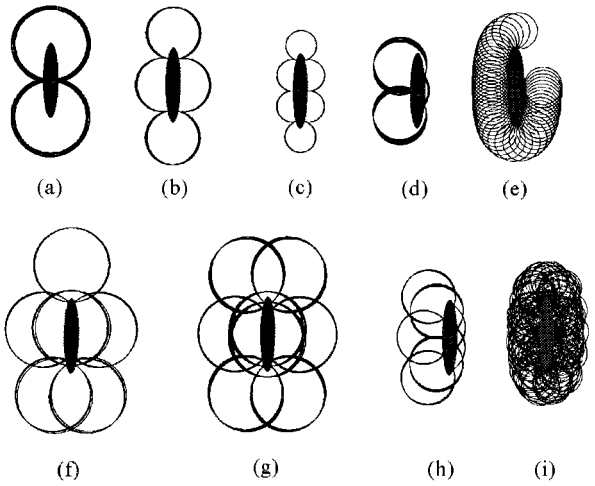

FIG. 3. Set of trajectories in real space. Trajectories (a), (b), (c), (d), (f), (g), and (h) correspond to periodic and quasiperiodic orbits. Trajectory (i) is a chaotic trajectory, and (e) represents an anticlockwise orbit.

scattering on, for example, an impurity between two adjacent antidots. One therefore expects an increase in the resistivity at values of the magnetic field, where the Poincaré sections show that a large part of the phase space consists of stable orbits.

C. Lyapunov exponent

To obtain a better quantitative description of the effects on the resistivity from the qualitative understanding extracted from the Poincaré sections, we now compute the Lyapunov exponents, which characterize the sensitivity of the system to the initial conditions.[18] A chaotic system is characterized by an exponential divergence of two closed trajectories in the phase space as time evolves. To compute the exponent of this divergence, the method proposed by Benettin and Strelcyn has been used.[20] Starting with two closed trajectories separated by e_i in phase space, one calculates the separation e_{i+1} after one collision, and rescales it to the original length e_i. Then, after N collisions, the Lyapunov exponent can be approximated by

$$\lambda = \frac{1}{t}\sum_{i=0}^{N-1} \ln\left(\frac{e_{i+1}}{e_i}\right).$$

λ, which represent the maximum Lyapunov exponent per unit time, has several important properties: the limiting value of λ is independent of the size and the sign of e_i (as long as e_i is quite small compared to the dimension of the billiard), and λ is constant over a given stochastic component.

Due to the fact that each scattering event leads to an increased separation of the two trajectories, we have modified the definition, so that the maximum Lyapunov exponent is calculated per scattering event instead of per unit time. It is then possible to compare λ for the whole range of the magnetic field. Thus a stable orbit corresponds to a low value of λ ($\lambda \to 0$), whereas a chaotic orbit corresponds to a higher value ($\lambda \gg 0$). Although the exponent is defined for an infinite number of iterations, it is found that after 3000 collisions λ has reached its limiting value.

As λ depends on the initial condition, it has been calculated by dividing the phase space into a grid of 1280 rectangles, each one representing an initial condition. Because of the symmetry of the billiard, we are only interested in the range $\theta[0°,90°]$ and $\gamma[0°,160°]$. The calculations have been stopped at $\gamma = 160°$, because at higher values only the anticlockwise orbits remains which do not have any physical significance. Figure 4 shows maps of the calculated λ for four values of the magnetic field. Due to the discretization of the initial conditions, smooth and contour detection algorithms have been employed. A regular behavior of the orbits is characterized by a value of the Lyapunov exponent close to zero (dark areas on the map). These stability islands ($\lambda \to 0$), which are surrounded by a chaotic sea ($\lambda \gg 0$), are associated with the formation of quasiperiodic and periodic orbits, i.e., two (quasi)closed trajectories will remain in the same vicinity in the space phase. By increasing the magnetic field, a sweep is made through the different periodic trajectories plotted in Fig. 3. As deduced from the Poincaré section, the chaotic component increases with the magnetic field, and for $\alpha = 12$ it covers the entire phase space. Only the anticlockwise orbits remain for $\gamma \to 160°$ (cf. Fig. 3). Over the chaotic sea, λ has a nearly constant mean value (within small fluctuations) independently of the degree of magnification of the initial grid, revealing in some sense the universal scaling behavior of the chaotic component.

The main interest of this billiard is the possibility, for certain magnetic fields, to have both regular and chaotic components in the phase space. Thus an important quantity that plays a dominant role in the comprehension of the experimental results is the fraction of periodic orbits, representing the probability of an electron having a regular motion. Practically, this quantity is computed by counting the number of orbits having a value of $\lambda \leqslant \lambda_{\text{crit}}$.[23]

D. Electric field

To approach the experimental situation, the evolution of the system has to be studied in the presence of an applied electric field. Due to the magnetic field, in the absence of an electric field, the particle remains trapped around the billiard and cannot escape. This situation can be changed by the drift force which results from an applied electric field. Thus the particle has the possibility to leave the billiard, preventing us from calculating the Lyapunov exponent and the Poincaré section. The evolution of the system can instead be analyzed by studying the number of collisions the particle makes with the boundary before escaping. In contrast to a chaotic trajectory in the phase space, stable orbits will not be affected by a low electric field. This can be related to the Kolmogoroff-Arnold-Moser theorem,[18] where the electric field acts as a small perturbation of the Hamiltonian system. This intuitive result is demonstrated in Fig. 5, where the number of collisions as a function of the initial values has been calculated for a normalized value of the electric field $\varepsilon = \Gamma/L = 11 \times 10^{-3}$ for $\alpha = 2.8$. Here L is the length of the ellipse, and $\Gamma = m^*E/eB^2$ is the distance by which the orbit is translated by the electric field in one period.[24] The value of ε used here corresponds to a reasonable experimental value of the voltage applied over the microstructure. For computational reasons the number of collisions has been limited to

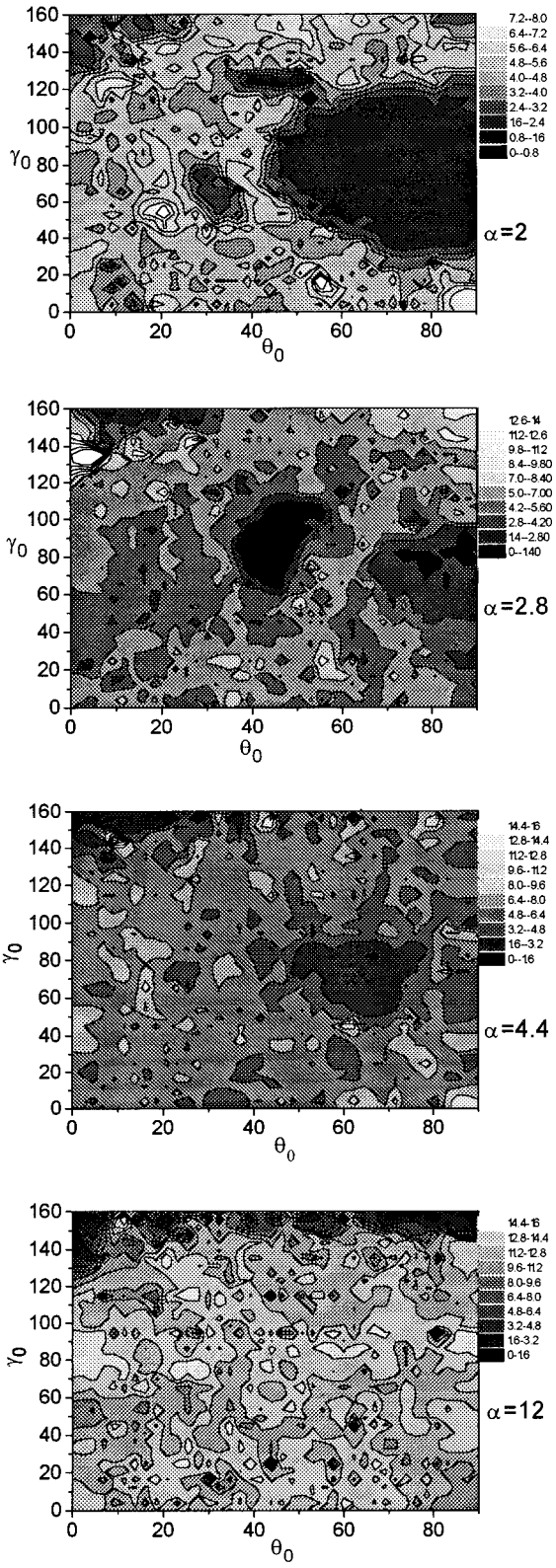

FIG. 4. Calculated maps of the Lyapunov exponent per unit of collision for four values of the magnetic field α. Dark areas represent stability islands and light areas represent chaotic seas.

8000. As can be seen in Fig. 5, for such small values of ε, periodic orbits corresponding to pinned trajectories remain present in the phase space. The islands representing trajectories with more than 8000 collisions are surrounded by a sea

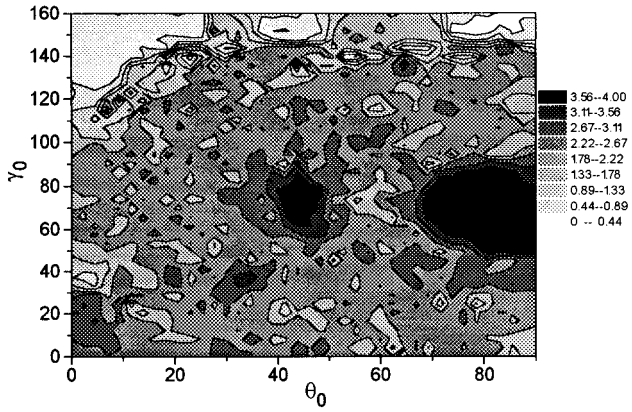

FIG. 5. Calculated number of collisions (log scale) as a function of the initial condition in a crossed electric and magnetic field ($\alpha=2.8$ and $\varepsilon=11\times10^{-3}$). Long scattering times are represented by dark areas and low times by light areas.

of low collision events. By identifying these with the stability islands and the chaotic sea in the Lyapunov exponent map (Fig. 4), we conclude that in the presence of an electric field, chaotic trajectories escape quickly from the billiard in contrast to periodic or quasiperiodic trajectories, that have a longer dwell time (the slight shift in the position of the stability island is due to the electric field which modifies the size of the cyclotron radius). This difference in behavior between chaotic and stable trajectories should be experimentally observable. As intuitively expected, the anticlockwise orbits are destroyed by the electric field.

Although the application of a small electric field breaks the symmetry of the billiard, rendering it anisotropic, the calculations have been checked for other directions of the electric field, and it has been found that the essential properties remains unchanged. Of course, for a sufficiently strong electric field, all the pinned orbit are destroyed and a particle that arrives will be reflected away. The system has turned completely to chaotic motion.

Apart from the drift motion produced by an electric field, there is a second mechanism that can eject an electron from the trajectory around the antidot: scattering on an impurity between two adjacent antidots. This can be included in the calculations as a long-time cutoff for the orbit. As mentioned previously, periodic orbits occupy a well-defined region of the real space, leading to a lower probability of scattering at an impurity, in contrast to a chaotic trajectory which fills the space between two antidots.

The electric-field-induced escape rate from an antidot for chaotic trajectories has been calculated, and we find an exponential law, i.e., the number of trapped chaotic orbits decreased with time as

$$N(t)=N(t_0)\exp(-\eta t),$$

where η is the classical escaping rate.[21,22] Further calculations have to be performed, notably to take into account the dependence of η on the electric and magnetic fields.

E. Experimental consequences

In previous sections, we showed that scattering around a single elliptically shaped antidot result in the presence of

both periodic and chaotic orbits. Computations of Poincaré sections and Lyapunov exponents can be used to give a quantitative information on the stability of these periodic orbits. A small electric field destroys the chaotic orbits, but does not affect the pinned (clockwise) orbits. As previously proposed,[4,5] the escaping particle will contribute to the conductivity, and, thus, a maximum in the number of pinned orbits will correspond to a maximum in the resistivity. Fleischmann, Geisel, and Ketzmerick[5] have calculated the magnetoresistance of a square lattice of circular antidots using classical linear-response theory. The problem can be decomposed into two parts: the calculation of the fraction of pinned orbits in phase space (which exhibits maxima corresponding to orbits enclosing a number of antidots) and the calculation of the velocity correlation function averaged over phase space. As they considered a particle encompassing the potential created by the antidot, and not a direct collision on the boundary (the dynamics of a particle colliding with a circular antidot is regular, and does not show any chaotic component), the mechanism of pinning in the present case is of course very different. Here the correlation function is nontrivial to calculate, since the electron trajectories cannot be followed once they leave the antidot. Experimentally, the system consists of a lattice of oval antidots, and the trajectories through the complete lattice, and not only around a single antidot, have to be taken into account. However, by calculating the area in the phase space, for which the number of collisions is larger than the cutoff number given by the elastic-scattering time, the fraction of periodic orbits can in principle be obtained. This number gives information as to the position of the maxima in the magnetoresistance. Although most of the pinning mechanisms have been attributed to particles surrounding or colliding with a group of antidots,[25] our calculations indicate that a carrier can be trapped by a single antidot, and thus an array of antidots with chaotic shapes should present similar magnetoresistance oscillations. Since the cutoff may not be trivial to obtain, as the scattering probability depends on the portion of real space covered by the trajectories, and since we have seen that a small electric field has very little effect on the phase-space maps (neglecting the physically meaningless anticlockwise orbits), we have instead calculated the fraction of periodic orbits from the Lyaponov exponent maps. The error in the positions of the extrema in the fraction of periodic orbits that this simplification introduces is expected to be small, and due mainly to the slight modification of the cyclotron radius brought about by the electric field. The amplitude might be somewhat altered: as the cyclotron radius decreases with increasing magnetic field, the real space covered by the orbits will decrease, and hence the probability of impurity scattering will also decrease. This may lead to a smaller amplitude of the peaks at low magnetic field compared to those at high magnetic field.

III. EXPERIMENTAL RESULT AND DISCUSSION

A. Experimental details

To test the trapping mechanism experimentally, the magnetoresistance of an AlGaAs/GaAs heterostructure with a 2 DEG and a lateral lattice containing oval-shaped antidots was measured. The lattice was fabricated using electron-beam lithography and reactive plasma etching. To suppress scattering between adjacent antidots, the periodicity has been chosen to be quite large, $\simeq 2\ \mu$m. The properties of the original $Al_xGa_{1-x}As/GaAs$ were a mobility of $\mu = 2.5\times 10^5$ $cm^2\ V^{-1}\ s^{-1}$ with a mean free path $le = 2\ \mu$m. The geometrical length of the antidots is $L = 2a = 0.6\ \mu$m and $2b = 0.07\ \mu$m, leading to a ratio $\beta = a/b \simeq 8.5$. If we take into account the depletion area around each antidot, then β approaches the value $\beta = 5$ (a value of the depletion region equal to $0.05\ \mu$m is commonly accepted). To suppress geometrical resonances between adjacent antidots[25] as well as runaway trajectories, and in order to average over the initial conditions, the oval antidots were misoriented using a random number generator. Furthermore, to avoid any mesoscopic phenomena (such as universal conductance fluctuations), a macroscopic number of antidots were created ($\approx 10^5$), so that the lattice size is much larger than the coherence length. A schematic of the lattice is shown in Fig. 6. A second sample with a periodicity of $0.8\ \mu$m and an antidot length of $0.5\ \mu$m shows similar oscillations. For clarity, as the lower periodicity hinders the developments of orbits at the lowest magnetic fields, restricting the range over which the fluctuations can be observed, we compare the calculations only with the measurements of the more open sample (periodicity $2\ \mu$m). Before patterning the antidot, the 2DEG magnetoresistance did not show any oscillations.

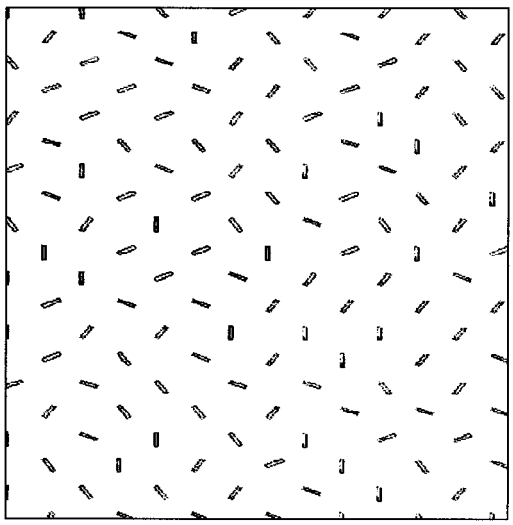

FIG. 6. Schematic view of the antidot lattices created by two interpenetrating square lattices of period $2\ \mu$m with one lattice shifted by $1\ \mu$m with respect to the other. The semiaxes of the elliptic antidots are 0.6 and 0.07 μm, respectively. The antidots have been misoriented using a random number generator.

The measurements were performed in a dilution refrigerator at a temperature $T = 50$ mK, using standard lock-in techniques with a current of a few nA and a frequency of 6.7 Hz. A magnetic field was applied by means of a superconducting magnet. Figure 7 shows the resistance of the sample as a function of the magnetic field. Reproducible fluctuations (both in repeated measurements and after thermal cycling) are observed for low values of the magnetic field. Beyond 0.7 T, Shubnikov–de Haas oscillations appears as classical

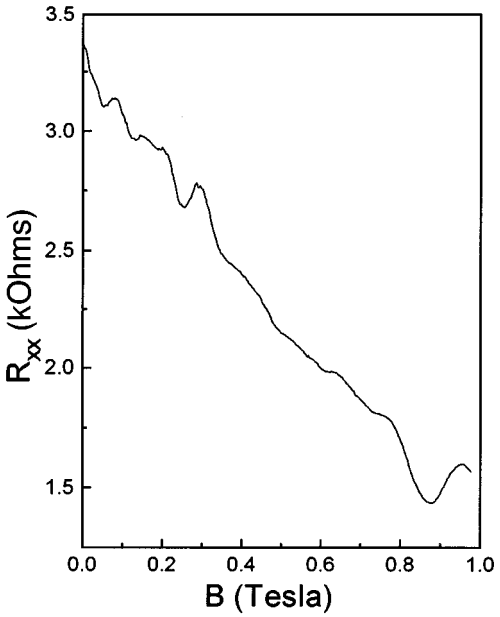

FIG. 7. Resistance of the sample as a function of the magnetic field at $T=50$ mK.

mechanics becomes inadequate. We believe the origin of the anomalous peaks at low field is due to periodic orbits developing around single antidots.

B. Discussion

To compare these experimental results qualitatively with the calculations, the calculated fraction of periodic orbits $P(\alpha)$ and the resistivity as a function of the normalized magnetic field α are plotted in Fig. 8. For clarity, the background resistivity has been removed by subtracting a second-order polynomial fit. Arrows indicate the position of the main peaks and troughs observed. The data clearly show the oscillatory structure predicted by our numerical calculations, even if some peaks are slightly shifted. The shift is more important for the low magnetic-field peaks corresponding to the largest cyclotron radius, which is to be expected, since these trajectories will be much more influenced by interference

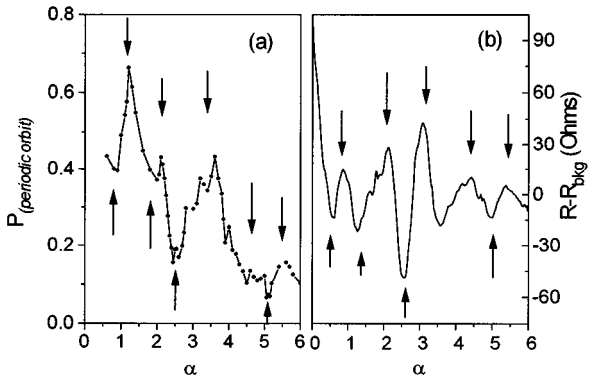

FIG. 8. Calculated fraction of periodic orbits in the phase space for an elliptic billiard (a) compared to the magnetoresistance observed in a 2DEG array of oval antidots (b). The arrows indicate peaks and troughs. To remove the background for (b), we subtracted a second-order polynomial.

effects from nearby orbits (drifting orbits and orbits trapped on neighboring antidots). Weiss *et al.*[4] proposed that three kinds of trajectories can develop in an array of artificial scatters: pinned orbits, drifting orbits, and scattered orbits. Pinned orbits localize the electron, and lead to peaks in the magnetoresistance, while drifting and scattered orbits contribute to the carrier propagation in the array. In our very open samples, with randomly disoriented elliptic antidots, the situation is somewhat different. Scattered orbits, imagined as balls in a pinball game, do not develop in the magnetic-field range of the anomalous resistance oscillations, but only play an important role when the size of the cyclotron radius is larger than the value of the mean spacing between two adjacent antidots ($\alpha \leqslant 1$ for our sample). Drifting orbits are likely to be scattered by impurities well before they have traversed the lateral superlattice. It is therefore likely that there is a strong mixing between drifting orbits and the trajectories around antidots, studied here. The drifting orbits supply electrons to the trapped orbits, and it is the escape from the trapped orbits which dominates the conductivity. Instead of pinned orbits around a number of antidots (which are unlikely to be very stable, due to the misorientation of the ellipses) our system can sustain two types of trajectories around a single antidot: those that stay trapped for a long time around a single antidot, and chaotic orbits that quickly escape, and together with drift orbits contribute to the conductivity. An incoming electron will have the probability $P(\alpha)$ to stay trapped and $1-P(\alpha)$ to escape quickly from the antidot. Thus the mechanism of propagation will be a succession of collisions around an elliptic antidot, with a dwell time which is a function of the fraction of the pinned orbit in the phase space. Fluctuation in $P(\alpha)$ will hence lead to fluctuations in the resistivity, and information on the dynamics of an electron around a single antidot is directly reflected in the resistivity of the macroscopic samples in crossed electric and magnetic fields. We should emphasize that it is only possible to compare the position of these fluctuations and not their absolute amplitude, the background resistance being governed mainly by elastic scattering on the impurity potential present between adjacent antidots.

Notice that there is no adjustable parameter for the calculated fraction of periodic orbits. An important difficulty lies in the estimation of the depletion area around each antidot, i.e., in the ratio β. A variation of the geometric ratio β changes the dynamics slightly, and leads to small changes in the fraction of periodic orbits. On the other hand, even if the antidots are not perfectly elliptically shaped, it has been shown in accordance with the KAM theorem that small deformations of the shape of the boundary of the billiard do not destroy the periodic trajectories.[17] Thus the inevitable variation in the shape of the antidots should not result in any dramatic experimental consequences. Another problem is that the electric field shifts the position of the peaks, due to small changes in the size of the cyclotron radius. Nevertheless, an approach based on calculating the fraction of periodic orbits agrees quite well with the experimental results, and confirms the role played by pinned orbits in transport.

In the presented calculations, only a hard-wall potential has been considered, leading to a specular condition of reflection, i.e., only the component of the velocity normal to the boundary is inverted. A more detailed analysis should of

course take into account a more realistic potential, but we do not believe that the dynamics would be dramatically changed.[26] Classically, in the case of a smoother potential, a shift in the outgoing trajectory has to be taken into account. This means that the angle is conserved during a collision, but the outgoing trajectory is shifted slightly back with respect to the incoming one. We should also comment that studies on antidot superlattices[4,5] have shown a large difference between hard-wall and soft-wall potentials. However, these studies were made on lattices with small periodicities, so that the extent of the potential could significantly affect the real space available for the electron trajectories. Here the lattice is sufficiently open, that such considerations are unimportant.

Even though a quantitative comparison between the macroscopic and the local electric field is difficult to make, the measured electric-field dependence (not shown) seems to follow the calculations. The unchanged Shubnikov–de Haas oscillation at higher magnetic field for higher electric fields may indicate that the destruction of the fluctuation at high values of the electric field is not a heating effect, but rather due to the disappearance of the periodic orbits. However, further experiments on the electric-field dependence are clearly needed to draw any firm conclusions.

IV. CONCLUSION

The chaotic dynamics of the trapping of a charged particle around an artificial impurity in a magnetic field has been studied both theoretically and experimentally. Numerical calculations, using a magnetic billiard model, show that periodic and chaotic orbits can coexist as an electron collides on the convex side of an elliptically shaped antidot. The situation is different from that of a stadium billiard inside a concave microstructure, in that the system here is open. However, the study of Poincaré sections and the Lyapunov exponent over the whole phase space allow us to calculate the fraction of the phase space containing periodic orbits. It is shown that the periodic orbits are not affected by the perturbation of a small electric field, in contrast to the chaotic trajectories which quickly escape from the antidot. Thus this fraction can be related to the magnetoresistance, and shows oscillations as a function of the magnetic field. In order to make a comparison with a real experimental system, the low-field magnetoresistance of an array of elliptically shaped antidots created in a 2DEG has been measured. Observed oscillations in the resistance are consistent with the numerically calculated fraction of periodic orbits, and confirm that electrons in a magnetic field can be trapped colliding around a single antidot. These magnetoresistance oscillations are different in nature from commensurability oscillations observed in samples with lattices of circular antidots, in that they rely on collisions with the artificial impurity, and the mixture of both chaotic and periodic orbits in phase space. In fact, they cannot be observed in a lattice of circular antidots, since these only sustain periodic orbits trapped around an antidot, that do not show a large difference in trapping dwell time.

ACKNOWLEDGMENTS

We thank Felix Von Oppen, Henrik Bruus, and Klaus Ensslin for helpful discussions. G.M.G was supported by Conselho Nacional de Desenvolvimento Cientifico e Tecnologica (CNPq). This work was supported by CNRS (France), CNPq, Fundação de Amparo à Pesquisa do Estado de São Paulo (Brazil), and Comité Français d'Evaluation de la Coopération Universitaire avec le Brésil.

[1] C. W. J. Beenakker and H. van Houten, in *Solid State Physics*, edited by H. Ehrenreich and D. Turnbull (Academic, San Diego, 1991), Vol. 44, p. 1, and references cited therein.

[2] E. Heller, Phys. Rev. Lett. **53**, 1515 (1984).

[3] H. Baranger, R. A. Jalabert, and A. D. Stone, Phys. Rev. Lett. **70**, 3876 (1993).

[4] D. Weiss, M. L. Roukes, A. Mensching, P. Grambow, K. von Klitzing, and G. Weimann, Phys. Rev. Lett. **66**, 2790 (1991).

[5] R. Fleischmann, T. Geisel, and R. Ketzmerick, Phys. Rev. Lett. **68**, 1367 (1992).

[6] E. M. Baskin, G. M. Gusev, Z. D. Kvon, A. G. Pogosov, and M. V. Entin, Pis'ma Zh. Éksp. Teor. Fiz. **55**, 649 (1992) [JETP Lett. **55**, 678 (1992)].

[7] I. V. Zozoulenko, F. A. Maaø, and E. H. Hauge, Phys. Rev. B **53**, 7975 (1996).

[8] G. M. Gusev, P. Basmaji, D. I. Lubyshev, L. V. Litvin, Yu. V. Nastaushev, and V. V. Preobrazhenskii, Phys. Rev. B **47**, 9928 (1993).

[9] K. Tsukagoshi, M. Haraguchi, S. Takaoka, and K. Murase, J. Phys. Soc. Jpn. **65**, 811 (1996).

[10] G. M. Gusev, P. Basmaji, Z. D. Kvon, L. V. Litvin, Yu. V. Nastaushev, and A. T. Toporov, J. Phys. Condens. Matter **6**, 73 (1994).

[11] M. V. Budantsev, Z. D. Kvon, A. G. Pogosov, A. E. Plotnikov, N. T. Moshegov, and A. I. Toropov, Pis'ma Zh. Éksp. Teor. Fiz. **63**, 336 (1996) [JETP Lett. **63**, 347 (1996)].

[12] M. C. Gutzwiller, *Chaos in Classical and Quantum Mechanics* (Springer, New York, 1990).

[13] O. Meplan, F. Brut, and C. Gignoux, J. Phys. A **26**, 237 (1993).

[14] Zhen-Li Ji and K. F. Berggren, Phys. Rev. B **52**, 1745 (1995).

[15] M. Robnik and M. V. Berry, J. Phys. A **18**, 1361 (1985).

[16] C. M. Marcus, A. J. Rimberg, R. M. Westervelt, P. F. Hopkins, and A. C. Gossard, Phys. Rev. Lett. **69**, 506 (1992).

[17] M. Robnik, J. Phys. A **16**, 3971 (1983).

[18] R. C. Hilborn, *Chaos and Nonlinear Dynamics* (Oxford University Press, New York, 1994).

[19] This transition occurs when two closed trajectories in phase space can no longer separate. Practically, a geometrical criterion is when the cyclotron radius becomes close to the minimum radius of curvature of the ellipse, i.e., $Rc \leqslant \rho_{0\min} = b^2/a$.

[20] G. Benettin and J. M. Strelcyn, Phys. Rev. A **17**, 773 (1978).

[21] Such an exponential law is similar to what has been obtained for a chaotic ballistic cavity, where $N(t)$ is the number of electrons present in the cavity after a time t.

[22] R. A. Jalabert, H. U. Baranger, and A. D. Stone, Phys. Rev. Lett **65**, 2442 (1990).

[23] The choice of this value is made by looking at the distribution of the Lyapunov exponent over the phase space. The value of λ_{crit} corresponds to the separation between the regular and chaotic components.

[24] S. A. Trugman, Phys. Rev. Lett **62**, 579 (1989).

[25] G. M. Gusev, Z. D. Kvon, Yu. V. Nastaushev, L. V. Litvin, A. K. Kalagin, and A. I. Toropov, Superlatt. Microstructures **13**, 383 (1993).

[26] V. Nikos Nicopoulos and S. A. Trugman, Phys. Rev. B **45**, 11 004 (1992).